A Metastable Intermediate State of Microtubule Dynamic Instability That Differs Significantly between Plus and Minus Ends

P.T. Tran,* R.A. Walker,‡ and E.D. Salmon*

*Biology Department, University of North Carolina, Chapel Hill, North Carolina 27599-3280; and ‡Biology Department, Virginia Polytechnic Institute and State University, Blacksburg, Virginia 24061-0406

Abstract. The current two-state GTP cap model of microtubule dynamic instability proposes that a terminal crown of GTP-tubulin stabilizes the microtubule lattice and promotes elongation while loss of this GTP-tubulin cap converts the microtubule end to shortening. However, when this model was directly tested by using a UV microbeam to sever axoneme-nucleated microtubules and thereby remove the microtubule's GTP cap, severed plus ends rapidly shortened, but severed minus ends immediately resumed elongation (Walker, R.A., S. Inoué, and E.D. Salmon. 1989. *J. Cell Biol.* 108: 931–937).

To determine if these previous results were dependent on the use of axonemes as seeds or were due to UV damage, or if they instead indicate an intermediate state in cap dynamics, we performed UV cutting of self-assembled microtubules and mechanical cutting of axoneme-nucleated microtubules. These independent methods yielded results consistent with the original work: a significant percentage of severed minus ends are stable after cutting. In additional experiments, we found that the stability of both severed plus and minus ends could be increased by increasing the free tubulin concentration, the solution GTP concentration, or by assembling microtubules with guanylyl-(α,β)-methylene-diphosphonate (GMPCPP).

Our results show that stability of severed ends, particularly minus ends, is not an artifact, but instead reveals the existence of a metastable kinetic intermediate state between the elongation and shortening states of dynamic instability. The kinetic properties of this intermediate state differ between plus and minus ends. We propose a three-state conformational cap model of dynamic instability, which has three structural states and four transition rate constants, and which uses the asymmetry of the tubulin heterodimer to explain many of the differences in dynamic instability at plus and minus ends.

Dynamic instability is the ability of a microtubule end to abruptly and stochastically switch between persistent phases of elongation and rapid shortening (Mitchison and Kirschner, 1984). In the cell, microtubule dynamic instability is important for a number of microtubule-based processes (for review see Inoué and Salmon, 1995), including cell morphogenesis (Kirschner and Schulze, 1986), organelle motility (Inoué and Salmon, 1995), mitotic spindle formation (Hyman and Karsenti, 1996), and chromosome movement (Rieder and Salmon, 1994; Inoué and Salmon, 1995). During the elongation phase of dynamic instability, tubulin association dominates, and thousands of dimers may add before a "catastrophe" occurs and the end switches abruptly to rapid shortening. During rapid shortening, thousands of dimers may dissociate from an end before a "rescue" occurs and the end converts back to the elongation phase. Both plus and minus ends of a microtubule exhibit dynamic instability, but they differ in both their kinetic rate constants of elongation and shortening and in the frequencies of catastrophe and rescue (Walker et al., 1988). For microtubules assembled from pure tubulin in vitro, plus ends typically grow faster than minus ends, but minus ends typically shorten faster than plus ends. Catastrophe is more frequent at plus ends, but rescue is more frequent at minus ends.

The currently accepted mechanism for microtubule dynamic instability at either plus or minus ends is the "GTP cap" model (for reviews see Caplow, 1992; Erickson and O'Brien, 1992; Inoué and Salmon, 1995; Erickson and Stoffler, 1996). Although both α and β tubulin bind GTP, only the GTP bound to β tubulin undergoes hydrolysis and exchange. It has been well established that tubulin αβ heterodimers with GTP bound to the β subunit (termed GTP-tubulin) makes stable additions to the end of an elongating microtubule and that the β GTP is subsequently hydrolyzed within the core of the microtubule. The GTP cap model postulates that this hydrolysis produces a labile "core" of GDP-tubulin subunits "capped" at

Address all correspondence to E.D. Salmon, Biology Department University of North Carolina, Chapel Hill, NC 27599-3280. Tel.: (919) 962-2265. Fax: (919) 962-1625.

the growing end by newly added GTP-tubulin. A catastrophe occurs when this GTP cap is lost, allowing the labile GDP-tubulin to rapidly dissociate. Rescue is proposed to occur when a shortening end is recapped with GTP-tubulin, which infrequently occurs in comparison to the rate of GDP-tubulin dissociation. Once in solution, β tubulin GDP is replaced with GTP, and the dimer is ready for assembly.

Support for this GTP cap model includes the following: (*a*) The great majority of the microtubule lattice is GDP-tubulin (Carlier and Pantaloni, 1981; Melki et al., 1990; Stewart et al., 1990); (*b*) elongation and shortening are distinctly different kinetic phases (Walker et al., 1988; Fygenson et al., 1994); (*c*) microtubules assembled with a slowly hydrolyzable analog of GTP, guanylyl-(α,β)-methylene-diphosphonate (GMPCPP),[1] are stable and do not exhibit dynamic instability (Hyman et al., 1992; Caplow et al., 1994; Caplow and Shanks, 1995, 1996; Tran et al., 1997); (*d*) GDP-tubulin subunits do not support elongation and promote catastrophe in buffers that permit dynamic instability (Jameson and Caplow, 1980; Caplow and Shanks, 1995; Vandecandelaere et al., 1995); (*e*) rapid shortening occurs within about 1 s at plus ends and within 4 s at minus ends when GTP-tubulin association is prevented by abrupt dilution (Voter et al., 1991; Walker et al., 1991); (*f*) a single layer of GMPCPP-tubulin appears capable of stabilizing microtubule ends to tubulin dilution (Drechsel and Kirschner, 1994; Caplow and Shanks, 1996); (*g*) dissociation during rapid shortening typically occurs at a constant velocity, with only a few hesitations, as expected for a homogeneous core of GDP-tubulin subunits (Walker et al., 1988; Billger et al., 1996); (*h*) energy from GTP hydrolysis is stored within the microtubule lattice and only released at shortening ends (Caplow et al., 1994); (*i*) the hydrolysis of β tubulin GTP within the microtubule produces a conformational strain in the tubulin dimer (Hyman et al., 1995; Melki et al., 1989); (*j*) the GDP microtubule core is less stiff than GMPCPP microtubules (Venier et al., 1994; Mickey and Howard, 1995); and (*k*) the structure of shortening ends is different than growing ends; growing ends exhibit "straight" or slightly curved protofilaments while shortening ends exhibit curved protofilaments whose length depends on the rate of rapid shortening (Erickson, 1974, 1975; Kirschner et al., 1974, 1975*a*,*b*; Simon and Salmon, 1990; Mandelkow et al., 1991; Chrétien et al., 1995; Erickson and Stoffler, 1996; Tran et al., 1997).

Although the GTP cap model appears to explain many aspects of dynamic instability at microtubule plus ends, it does not account for the stability of severed minus ends generated by UV cutting of elongating microtubules (Walker et al., 1989). The model predicts that severing an elongating end will produce plus and minus ends with exposed GDP-tubulin and that these ends should convert immediately to rapid shortening. Walker et al. (1989) used a UV microbeam to sever individual microtubules viewed by video-enhanced differential interference contrast (VE-DIC) light microscopy. They found that severed plus ends shortened as predicted by the GTP cap model, but severed minus ends did not. Instead, these minus ends resumed elongation at rates typical of minus ends. When a spontaneous catastrophe subsequently occurred, shortening proceeded through the previous site of severing without hesitation, suggesting that the UV exposure did not irreversibly alter the microtubule lattice.

In this paper, we have tested two possible explanations for the unexpected stability of severed minus ends. First, to test the possibility that microtubules nucleated from plus and minus ends of axoneme seeds in the Walker et al. (1989) experiments are structurally different, self-assembled microtubules were severed with a UV microbeam. Second, to test if UV ablation abnormally affects severed ends, hand-forged glass microneedles were used to sever microtubules mechanically by pressing them against the coverslip surface. In addition, we mechanically severed microtubules grown with Mg^{2+}-GMPCPP to test whether these severed ends are stable as predicted by the GTP cap model, and we examined the effects of GTP-tubulin and free Mg^{2+}-GTP concentrations on the stability of severed microtubule ends.

We conclude from these experiments that the differential stability of severed plus and minus ends is not an artifact but instead reveals an important metastable intermediate state between elongation and shortening at both ends of a microtubule. We propose that this metastable intermediate state is important in the regulation of microtubule dynamic instability and differs kinetically between plus and minus ends because of the polarized orientation of the tubulin αβ dimer in the microtubule lattice.

Materials and Methods

Tubulin and Axoneme Preparation

Tubulin was purified using the methods of Voter and Erickson (1984) and Walker et al. (1988). Briefly, porcine brain was homogenized and centrifuged through three cycles of warm–cold assembly–disassembly in PEM buffer (100 mM Pipes, 2 mM EGTA, 1 mM $MgSO_4$, pH 6.9) + 0.5 mM Mg^{2+}-GTP. All added GTP and GMPCPP in the present study are in a 1:1 ratio with $MgSO_4$, making them Mg^{2+}-GTP or Mg^{2+}-GMPCPP. The resulting pellets were resuspended in PEM buffer and passed over an ion exchange phosphocellulose column. The tubulin eluate was further purified by assembly at 37°C with 1 M Na-glutamic acid and then resuspended in PEM buffer containing 0.5 mM GTP and stored at −80°C. This was the stock GTP-tubulin used in all experiments. The concentration of the stock GTP-tubulin was measured with the BioRad protein assay kit (Hercules, CA), using BSA as a standard.

GTP-tubulin without excess Mg^{2+}-GTP in the buffer medium was made by passing the stock GTP-tubulin through a Sephadex G25 column to remove any excess nucleotides free in solution (O'Brien and Erickson, 1989). We pooled the middle fractions of the tubulin eluate to concentrate the tubulin and to assure that little excess Mg^{2+}-GTP was present. We verified that no free Mg^{2+}-GTP was present in the tubulin preparation by monitoring [^{32}P]GTP bound to tubulin and free [^{32}P]GTP eluted off in the excess buffer, as described by Caplow and Shanks (1995). The K_d for GTP-tubulin is 22 nM (Zeeberg and Caplow, 1979). This yields an equilibrium concentration of free Mg^{2+}-GTP of ~1 μM for 50 μM GTP-tubulin. Furthermore, the GTPase activity of unpolymerized phosphocellulose-purified tubulin is exceedingly low, less than 10^{-3} nmol of P_i/min/mg (David-Pfeuty et al., 1977). Thus, GTP-tubulin collected from the Sephadex column is effectively in a 1:1 complex, with little or no free Mg^{2+}-GTP. A portion of this eluate was used in experiments where low or no excess solution Mg^{2+}-GTP was required.

GMPCPP-tubulin was made by mixing the GTP-tubulin collected from the Sephadex column above to PEM buffer containing 1.5 mM Mg^{2+}-GMPCPP. At the high concentration of GMPCPP used, the exchangeable GTP on each tubulin dimer was effectively competed off and replaced by a GMPCPP, creating GMPCPP-tubulin (Hyman et al., 1992; Caplow et al., 1994).

1. *Abbreviations used in this paper*: E, I, and S, elongation, intermediate, and shortening states; GMPCPP, guanylyl-(α,β)-methylene-diphosphonate; VE-DIC, video-enhanced differential interference contrast.

Axonemes were purified using the method of Bell et al. (1982). Briefly, *Lytechinus pictus* sperm flagellar axonemes were osmotically demembranated in a 20% sucrose solution and separated from sperm heads with a homogenizer. Axoneme pellets were then washed in a low salt buffer (100 mM NaCl, 4 mM $MgSO_4$, 1 mM EDTA, 10 mM Hepes, 7 mM β-mercaptoethanol, pH 7.0), and dynein arms were removed by suspending pellets in a high salt buffer (600 mM NaCl, 4 mM $MgSO_4$, 1 mM EDTA, 10 mM Hepes, 7 mM β-mercaptoethanol, pH 7.0). Axonemes were further purified by sedimentation through an 80% sucrose solution. Purified axonemes were stored in 1:1 low salt/glycerol solution at −20°C. Before being used, axonemes were washed twice and resuspended in PEM buffer. All chemical reagents mentioned were supplied by Sigma Chemical Co. (St. Louis, MO).

Microtubule Dynamic Instability Assay

Individual microtubules were observed by the method of Walker et al. (1988). Briefly, purified tubulin was mixed with axonemes and GTP in PEM buffer to the final concentration of 16 μM tubulin, ~3×10^7 axonemes/ml, and 1 mM Mg^{2+}-GTP. A 5-μl sample of this preparation was added to a clean glass slide covered with a biologically clean 22-mm^2 coverslip and then sealed with valap (1:1:1 mixture of vasoline/lanolin/petrolatum) to prevent drying and to prevent local convection inside the sealed chamber. The chamber has a typical thickness of 10 μm. The slide preparation was maintained at 22°C on the microscope stage to induce microtubule nucleation and assembly on the axonemes. Axonemes adhered tightly to both the coverslip and slide chamber surfaces, while the outgrowing microtubules were tethered to them.

Microtubule dynamics were viewed by VE-DIC microscopy as described by Walker et al. (1988). Images were recorded on 3/4-inch U-matic tape by either a Sony Model TVO-9000 (Park Ridge, NJ) recorder or 1/2-inch SVHS using a Mitsubishi BV1000 model recorder (Cypress, CA).

Darkfield Microscopy and UV Cutting of Self-assembled Microtubules

For experiments involving severing self-assembled microtubules with a UV microbeam, tubulin was mixed with Mg^{2+}-GTP and PEM buffer to a final concentration of 30 μM tubulin and 1 mM Mg^{2+}-GTP. A 5-μl sample was then added onto a clean glass slide, covered with a biologically clean quartz coverslip, and then sealed with valap. The slide preparation was maintained at 22°C on the microscope stage to induce microtubule self-assembly. The assembled microtubules did not adhere to the slide or coverslip surfaces.

The experiment was done using darkfield microscopy to increase depth-of-field resolution to help visualize the freely fluctuating microtubules. A microscope (model Standard; Carl Zeiss, Inc., Thornwood, NY) was equipped with an HBO 100-W mercury arc lamp (model Osram; Bulb-Tronics, Farmingdale, NY), a darkfield condenser (Carl Zeiss, Inc.), and a 100×/0.85 NA glycerin immersion objective lens (model Ultrafluor; Carl Zeiss, Inc.). Images were projected with a 6.7× ocular (Nikon, Inc., Melville, NY) to a video camera (model SIT; Dage-MTI, Michigan City, IN). A second HBO 100-W mercury arc lamp served as the UV source. A quartz collector lens directed the lamp output through an adjustable diaphragm (the slit) and onto a dichroic mirror inserted in the filter carrier of an illuminator (model IV FL; Carl Zeiss, Inc.) mounted on top of the microscope. It was necessary to remove the glass telan lenses of the illuminator to permit transmittance of UV light. This required changing the light path above the filter carrier: the path length was shortened by ~65 mm so that the specimen image was projected to the intermediate image plane at the ocular field stop. The dichromatic mirror reflected wavelengths of <400 nm to the objective, which projected an image of the UV slit onto the specimen image plane. To focus and position the UV slit, UV blocking and neutral density filters were placed in the appropriate slots in the illuminator.

The shutter was opened to expose the microtubule to the UV microbeam, thereby severing the microtubule. Exposures of <1 s of the UV microbeam faithfully severed microtubules. Images were recorded on 3/4-inch U-matic tape by a Sony Model TVO-9000 recorder.

VE-DIC Microscopy and Glass Microneedle Severing of Axoneme-nucleated Microtubules

For mechanical severing of microtubules, glass microneedles (outer diameter 0.8 mm and inner diameter 0.6 mm) were hand-pulled from small Pyrex glass capillary tubes (Drummond Scientific, Broomall, PA). The capillary tubes were held over a small fire burner made from funneling house gas through a glass pipette and then quickly pulled while still hot to produce long fine needle tips. The needle tips were then forged using a micro-forge device (model A; Microforge de Fonbrune, Energy Beam Science, Inc., Agawam, MA) to produce a kink for efficient cutting. Typical cutting tips were 0.5 μm in diameter. A microneedle was attached to an Ellis piezoelectric micromanipulator (Begg and Ellis, 1979) and inserted into a Kiehart-Ellis slide chamber during each experiment (Kiehart, 1981). After each experiment, the needle was removed and cleaned with strong detergent (10% potassium dichromate).

The Kiehart-Ellis slide chamber was made to the specification of Kiehart (1981). It is essentially a metal slide with the center cut out to produce an opening. In our preparation, two biologically clean coverslips were placed on top and bottom of the metal slide and sealed with silicon grease to produce a 1-mm-high chamber opened on one side. This large chamber thickness was necessary to accommodate the insertion of the microneedle. A 5-μl sample of axonemes was first spread onto the bottom coverslip to cover a round area of ~4 mm in diameter. This procedure allowed for axoneme attachment to the inner glass surface. Mineral oil was then pipetted into the chamber to about two thirds of the chamber volume without touching the spot containing the axonemes. Purified tubulin was then mixed with Mg^{2+}-GTP in PEM buffer to a final concentration of 16 μM tubulin and 1 mM Mg^{2+}-GTP; 32 μM tubulin and 1 mM Mg^{2+}-GTP; or 2 μM tubulin and 1 mM Mg^{2+}-GMPCPP. A 25-μl sample of this preparation was then pipetted into the chamber on top of the axoneme-coated region. This volume formed a buffer column between the upper and lower coverslips. Mineral oil was then pipetted in to fill up the empty volume. The prepared Kiehart-Ellis slide chamber was maintained at 22°C on the microscope stage to induce nucleation and assembly of microtubules.

Imaging was done using a custom-built inverted microscope equipped with DIC optics, a 100×/1.25 NA oil immersion objective lens (model Plan; Carl Zeiss, Inc.) and 1.4 NA condenser, a 100-W HBO mercury arc lamp, and an Ellis fiber-optic scrambler as illumination source (Walker et al., 1990). Images were further enlarged with 1.6 optivar and a 4× projection tube leading to a video camera (model C2400 Newvicon; Hamamatsu Corp., Hamamatsu City, Japan). Images were enhanced with a video processor (mode Argus 10; Hamamatsu Corp.) and recorded onto S-VHS video cassette tape with a video cassette tape recorder (model BV1000 S-VHS; Mitsubishi).

The above apparatus setup was further modified with a peripheral attachment at the side of the specimen stage containing the Ellis piezoelectric micromanipulator (Begg and Ellis, 1979). A piezoelectric micromanipulator is superior to a mechanical micromanipulator by its ability to produce smooth and fast three-dimensional movements. A hand-forged glass needle with tip diameter of 0.5 μm was then placed onto the micromanipulator, and its tip was inserted into the specimen chamber. The severing motion was performed by positioning the needle tip over a microtubule and then quickly bringing the tip down, pressing the microtubule against the glass surface and severing it. Severing is a quick and smooth motion performed within <1 s duration.

To find and position the needle tip within the 25-μm-wide video field of view, we initially used the low magnification view provided by the telescope built into the microscope body tube of the vertical optical bench VE-DIC microscope (Walker et al., 1990). While viewing with the telescope, the needle tip was centered on the microscope axis and brought to within 25 μm of the coverslip. We then switched to normal viewing mode and used the joy-stick controller on the piezoelectric micromanipulator to bring the tip down to the coverslip surface. At the high contrast required to image a single microtubule, the needle produced tremendous "flare" in the video image. Fortunately, by orienting the video camera so that the needle extended into the image field from right-to-left, we reduced the flare along the axis of the needle without obscuring the image of microtubules to the left as well as above and below the needle tip.

A possible explanation of the efficient severing of a 25-nm-diam microtubule with a 500-nm-diam needle to produce "native" ends has been provided by Nicklas et al. (1989). Essentially, as the needle presses the microtubule against the coverslip surface, the microtubule lattice is distorted. This distortion exceeds the forces of the lateral and longitudinal associations of the tubulin subunits, and thus disrupts the bonds between subunits, thereby breaking the microtubule.

Data Analysis

For microtubules nucleated from axonemes, the rates of elongation and rapid shortening were measured from our tape recordings. We used a

computerized tracking analysis system to monitor the microtubule length changes over real time (Gliksman et al., 1992). A point cursor was electronically overlaid on the video screen and used to track the ends of the microtubules. Data points were taken by positioning the cursor with the mouse and clicking the mouse. Changes in the microtubule length were plotted as a function of time. Elongation and rapid shortening rates of microtubules were calculated from least squared regression analysis of the length versus time plots. The frequencies of catastrophe and rescue were determined by counting the number of switching events over the total time observed (Walker et al., 1988). All rates are given as mean ± SEM.

For self-assembled microtubules in the UV severing experiment, it was impossible to differentiate between plus and minus ends without a marker to compare their rate of elongation. Therefore, no polarity was assigned to the ends. Instead, we designated each severed end as stable if it continued growing or as unstable if it immediately shortened.

For axoneme-nucleated microtubules in the glass microneedle severing experiment, we measured elongation rates by the procedure described above and then assigned the faster growing end plus and the corresponding slower growing end minus.

Results

UV Microbeam Severing of Self-assembled Microtubules Demonstrated Asymmetrical Behavior between Plus and Minus Ends

To determine whether the asymmetry in the behavior of severed plus and minus ends observed in the UV cutting studies of Walker et al. (1989) was due to structural differences in microtubules nucleated from opposite ends of axonemes, self-assembled microtubules observed by darkfield microscopy were severed by a UV microbeam (Fig. 1). At 22°C, 30 μM tubulin and 1 mM Mg^{2+}-GTP, little self-assembly occurred, and the few microtubules that formed grew very long (>500 μm) after 30 min. After severing, the newly created ends remained within the plane of focus for long periods of time since each of the new microtubules were sufficiently long to limit the extent of Brownian motion (Fig. 2). The majority of the long self-assembled microtubules severed by the UV microbeam exhibited asymmetrical behavior. Analysis showed 103 out of 118 total irradiations (87.3%) produced one stable end which resumed growing, and one labile end which immediately began rapid shortening. Both severed ends converted to rapid shortening in about 10% of the irradiations, while both severed ends were stable in 2.5% of the irradiations (Table I). Although plus and minus ends cannot be identified by this method, the severed ends of self-assembled microtubules exhibited the same asymmetrical stability predicted by UV irradiation of axoneme-nucleated microtubules (Walker et al., 1989).

Glass Microneedle Cuttings of Axoneme-nucleated Microtubules Show Asymmetry between Plus and Minus End Behavior

To test whether the high energy UV microbeam was differentially affecting microtubule plus and minus ends, we assembled a mechanical cutting apparatus to sever microtubules (Fig. 3). We mechanically severed axoneme-nucleated microtubules by pressing them against the coverslip surface with a glass microneedle (Fig. 4). At 22°C and 16 μM tubulin and 1 mM Mg^{2+}-GTP, many microtubules nucleated and grew from the plus and minus ends of the coverslip-bound axonemes.

Each cut of a microtubule produced two new microtubules: one remained attached to the axoneme, and one quickly diffused out of view. Thus, we could clearly distinguish only whether the tethered severed ends were stable

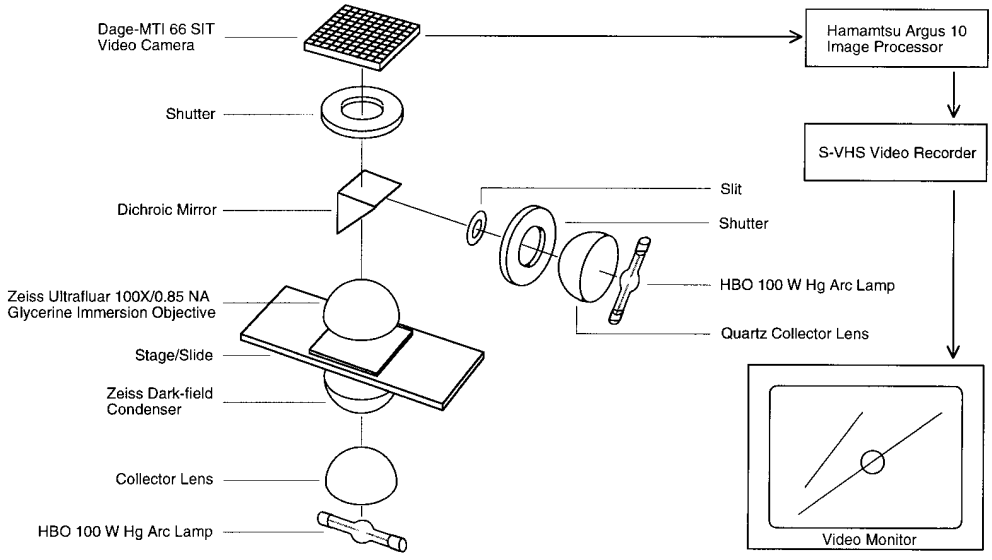

Figure 1. Schematic diagram of the darkfield UV microbeam apparatus. Self-assembled microtubules were observed by video darkfield microscopy using an HBO 100-W mercury arc lamp, a darkfield condenser (Carl Zeiss, Inc.), a 100×/0.85 NA glycerin immersion objective (Carl Zeiss, Inc.), and a camera (model 66 SIT; Dage-MTI, Inc.). An HBO 100-W mercury arc lamp served as the UV source. A quartz collector lens directed the lamp output through an adjustable diaphragm (the slit) and onto a dichroic mirror, which reflected wavelengths <400 nm to the Ultrafluar objective. The slit image was then projected by the objective onto the specimen image plane. Design details for the integration of the UV microbeam and the darkfield microscope are provided in the text.

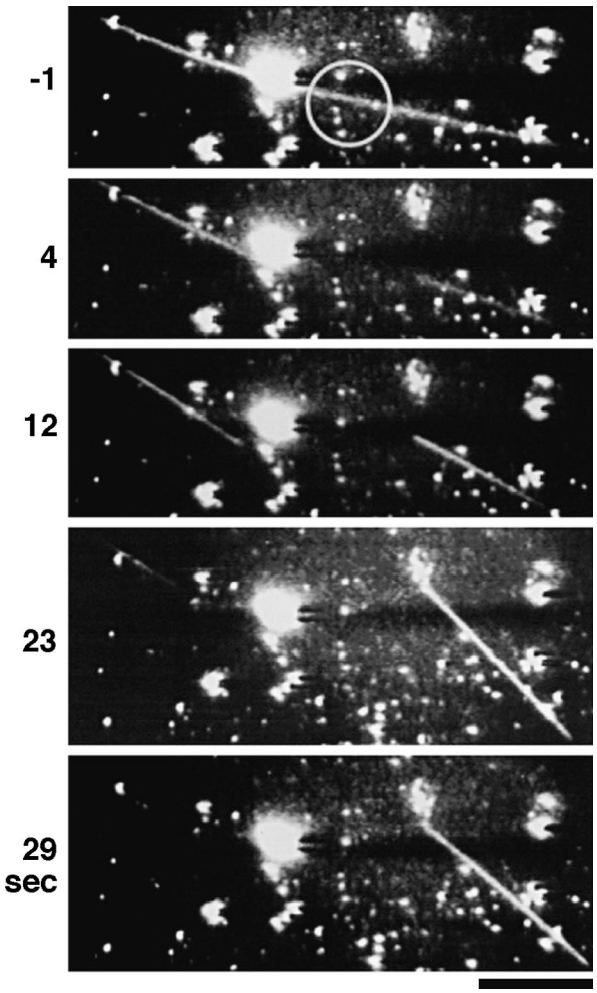

Figure 2. UV cutting of self-assembled microtubules. Microbeam irradiation of free microtubules produces two severed ends: typically one shortens, the other is stable. The microtubule shown extended out of the field of view for over 100 μm in either direction. The microbeam area is indicated by the circle. After irradiation, the severed end on the right is stable, and the severed end on the left shortened toward the left edge of the field through the observed time. Bar, 5 μm.

or unstable (Fig. 5). Furthermore, because microtubules were nucleated from axonemes, we could easily determine their polarity based on the threefold difference in elongation rate between the plus and minus ends and the 75-fold difference in rescue frequency between the minus and plus ends (Table II).

*Table I. Summary of UV Irradiation of Self-assembled Microtubules**

	n	Percentage of total
Microtubules irradiated	118	100
One end shortened and one end stable	103	87.3
Both ends shortened	12	10.2
Both ends stable	3	2.5

*Microtubules were self-assembled with 30 μM GTP-tubulin, 1 mM Mg^{2+}-GTP, at 22°C.

As with the UV experiment above, the majority of axoneme-nucleated microtubules severed by the glass microneedle exhibited asymmetrical behavior between plus and minus ends (Table III). At 16 μM free tubulin, analysis showed that 139 out of 140 severed plus end microtubules (99.29%) underwent immediate rapid shortening. These shortened completely back to the axoneme without rescue. At a later time, new microtubules renucleated and elongated at typical plus end rates. Only one severed plus end did not shorten, but instead continued growing at the same rate as it did before being cut. In comparison, 103 out of 132 severed minus ends (78.03%) did not shorten, but instead continued elongating. Of the 29 (21.97%) severed minus ends that did exhibit rapid shortening, all exhibited rescue after shortening for 2–3 μm, a behavior characteristic of minus but not plus ends at 22°C. Furthermore, the behavior of the severed plus and minus ends was not dependent on the position of the cut site along the whole length of the microtubule between the axoneme and the tip, as previously reported in the UV experiments (Walker et al., 1989).

To determine if GTP-tubulin concentration influences the stability of severed ends, we also severed microtubules grown at 32 μM tubulin and 1 mM Mg^{2+}-GTP. The percentage of severed plus and minus ends that were stable and did not immediately shorten increased (Table III). Analysis showed 40 out of 44 severed plus end microtubules (90.9%) underwent immediate rapid shortening, while four (9.1%) were stable and continued growing. In comparison, 55 out of 57 severed minus end microtubules (96.5%) did not immediately shorten. Instead, they continued growing; only two (3.5%) exhibited rapid shortening. Therefore, increasing the free tubulin concentration twofold (from 16 to 32 μM) led to an approximate 12-fold increase in the number of plus end microtubules that were stable after being severed and a 24% increase in the number of minus end microtubules that were stable. It should be noted that perfusion of growing plus and minus ends with buffer without tubulin results in both ends switching to rapid shortening within several seconds of tubulin dilution (Voter et al., 1991; Walker et al., 1991). Thus, the probability that either a severed plus or minus end will persist in elongation and not convert to rapid shortening depends on the concentration of free GTP-tubulin subunits.

Microtubules Assembled from GMPCPP-Tubulin Did Not Undergo Rapid Shortening after Being Mechanically Severed

The GTP cap model predicts that both ends of a microtubule are stabilized by the presence of a terminal crown of GTP-tubulin subunits (the cap). GMPCPP is a slowly hydrolyzable analog of GTP, and GMPCPP microtubules are stable to dilution and exhibit no rapid shortening phases (Hyman et al., 1992; Caplow et al., 1994). From a functional standpoint, a GMPCPP microtubule may be considered to have a continuous "GTP cap" along its entire length. To test this prediction, we nucleated 2 μM GMPCPP-tubulin from the ends of axonemes and severed the assembled microtubules by microneedle cutting. All newly exposed microtubule ends (74 plus ends and 49 minus ends) were stable after being severed with a microneedle (Table III),

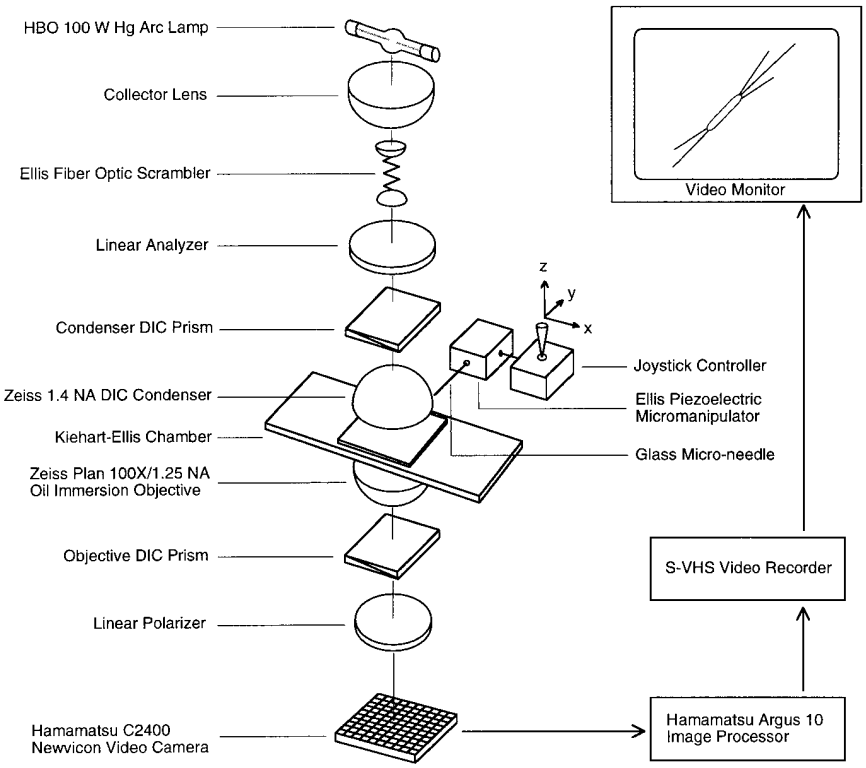

Figure 3. Schematic diagram of VE-DIC microscope setup for mechanical severing of single microtubules. Axoneme-nucleated microtubules were observed by VE-DIC microscopy using an HBO 100-W mercury arc lamp, a 100×/1.25 NA oil immersion objective (Carl Zeiss, Inc.), DIC condenser (Carl Zeiss, Inc.), DIC optics, and a video camera (model C2400 Newvicon; Hamamatsu Corp.) (Walker et al., 1990). The cutting apparatus consists of an aluminum Kiehart-Ellis chamber (Kiehart, 1981) and an Ellis piezoelectric cube attached to a joystick controller (Begg and Ellis, 1979).

independent of whether the microtubule was severed close to the growing tip or close to the axoneme. Thus, rapid shortening after microneedle cutting is not an artifact of the cutting process, but depends on the structure/chemistry of the microtubule lattice.

The Stability of Plus Ends Is Much More Sensitive than Minus Ends to Solution Mg^{2+}-GTP Concentration

All previously described experiments were carried out in the presence of 1 mM Mg^{2+}-GTP. To determine if free Mg^{2+}-GTP concentration plays a role in the stability of severed plus and minus ends, we attempted to mechanically cut axoneme-nucleated microtubules grown in the absence of added solution Mg^{2+}-GTP.

We created a tubulin preparation that is substantially depleted of free Mg^{2+}-GTP (~1 μM for 50 μM tubulin; see Materials and Methods) by passing the stock tubulin through a Sephadex G25 column (O'Brien and Erickson, 1989). GTP-tubulin, without added Mg^{2+}-GTP, was reported as able to support one round of polymerization (Carlier and Pantaloni, 1978; Carlier et al., 1987; O'Brien and Erickson, 1989). These investigators assayed microtubule polymerization by solution turbidity and thus could not distinguish between plus and minus end polymerization.

We found that no assembly occurred from axonemes (22°C) with 16 μM Sephadex-treated GTP-tubulin and no added Mg^{2+}-GTP. Only the minus ends of the axoneme fragments were observed to nucleate microtubules with 50 μM Sephadex-treated GTP-tubulin; no plus end nucleation and elongation occurred. The Sephadex-treated tubulin was not denatured since adding 1 mM Mg^{2+}-GTP to 16 μM Sephadex-treated tubulin produced normal plus and minus end elongation from the axoneme seeds. To test if depletion of Mg^{2+}-GTP induces catastrophe, we allowed both plus and minus end microtubules to grow initially at 20 μM GTP-tubulin and 1 mM Mg^{2+}-GTP and then perfused them through 50 μM Sephadex-treated GTP-tubulin with no added Mg^{2+}-GTP. The growing plus ends catastrophed during the perfusion and shortened back completely without rescue, while the minus ends continued growing.

We mechanically severed 106 growing minus end microtubules assembled with 50 μM Sephadex-treated tubulin and no added Mg^{2+}-GTP. Analysis showed that 76 out of 106 of the severed minus ends (72%) immediately shortened, but 30 out of 106 of the severed minus ends (28%) did not shorten but instead continued growing (Table III). The severed minus ends that rapidly shortened exhibited rescue and started regrowing after shortening an average of 3–4 μm in length, a length also exhibited at 16 μM GTP-tubulin and 1 mM Mg^{2+}-GTP (Walker et al., 1989).

Thus, the stability of both plus and minus ends depends on free Mg^{2+}-GTP. However, plus end stability is much more sensitive and critically dependent on Mg^{2+}-GTP, as also reported by Caplow and Shanks (1995), while at higher concentrations of Sephadex-treated GTP-tubulin, growing minus ends and a significant percentage of severed minus ends persist.

Discussion

A Metastable Intermediate State Exists between the Elongation and Shortening States of Dynamic Instability

Our results demonstrate that loss of the GTP-tubulin cap is necessary but not sufficient for rapid shortening. Sev-

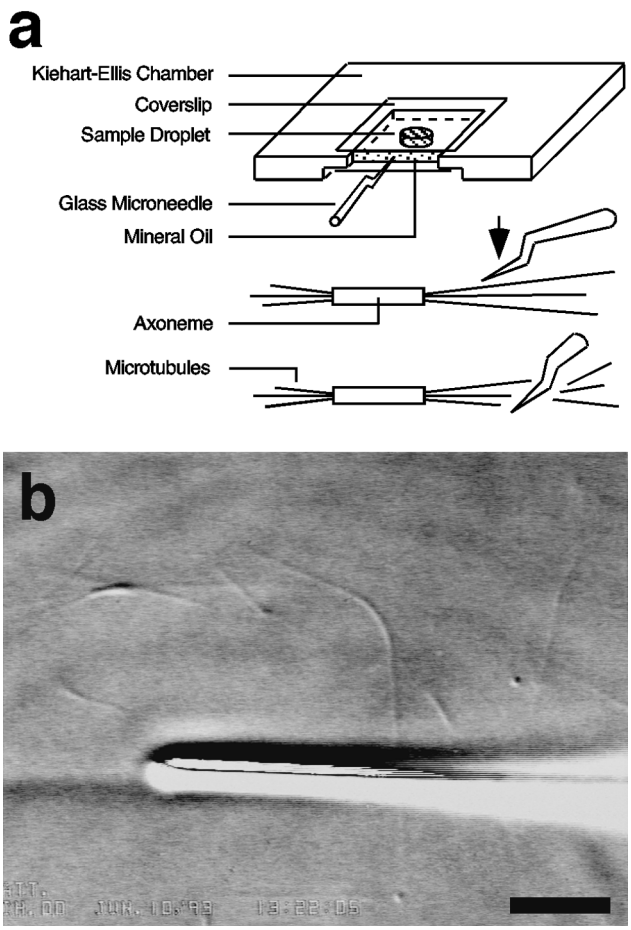

Figure 4. (*a*) Diagram of the Kiehart-Ellis chamber preparation, microneedle shape and alignment, and the mechanical severing motion. (*b*) Video image of the field of view. Shown is the glass microneedle tip pressing down on the coverslip surface and axoneme-nucleated microtubules. Bar, 5 μm.

ered plus and minus ends of microtubules assembled from GMPCPP-tubulin were stable as predicted by the GTP-tubulin cap model. However, under normal growth conditions where both growing plus and minus ends exhibit spontaneous catastrophe and dynamic instability (Walker et al., 1989), some severed plus ends and most severed minus ends did not shorten, but immediately resumed elongation at rates typical of unsevered ends. According to the GTP-tubulin cap model, severed ends of microtubules assembled from GTP-tubulin should immediately shorten because they are GDP-tubulin rather than GTP-tubulin ends.

It is unlikely that the stability of severed microtubule ends is due to unhydrolyzed GTP-tubulin or GDP-P_i embedded within the interior GDP-tubulin lattice: (*a*) No evidence has been found for the existence of GTP-tubulin within the microtubule lattice (for reviews see Caplow, 1992; Caplow and Shanks, 1996); (*b*) the existence and position of a stabilizing GTP cap has been localized to the terminal subunits (Stewart et al., 1990; Dreschel and Kirschner, 1994; Caplow and Shanks, 1996); (*c*) a complete ring of GTP-tubulin is necessary to block rapid shortening and induce rescue (Caplow and Shanks, 1996); (*d*) microtubules are not stabilized by elevated P_i concentrations (Caplow et al., 1989); and (*e*) the behavior of severed ends was similar for cut sites anywhere between the nucleation center and the growing end (Walker et al., 1989; this report).

Stable severed ends do not appear to be shortening ends that immediately rescue. Normally, at 22°C and 16 μM GTP-tubulin and 1 mM Mg^{2+}-GTP, plus ends in shortening rarely rescue, and minus ends shorten on average 3.5 μm (54,436 dimers) before a spontaneous rescue occurs (Table II). Thus, rescue is highly favored at minus ends. However, neither Walker et al. (1989) in their UV cutting studies nor we could see any detectable shortening of stable plus or minus severed ends within the resolution of our VE-DIC imaging system (about 350 nm or 560 dimers; Salmon et al. 1989). In addition, severing ends by either UV or mechanical cutting produced similar results, and thus possible effects of UV producing differential stabilization of minus ends (Walker et al., 1989) are ruled out. Our experiments also rule out the possibility that axoneme-nucleated plus end microtubules are somehow different from minus end nucleated microtubules. This possibility is unlikely since our experiments with self-assembled microtubules show that their severed ends exhibit similar behavior to the axonemal nucleated microtubules. Thus, the differential stability between plus and minus severed ends appears to be a fundamental property of microtubule polarity and not an artifact of the methods used to cut or assemble microtubules.

If a severed end is not a growing end (no GTP cap) and not a shortening end (no shortening), then there must be a metastable "intermediate" state between elongation and shortening states of dynamic instability with different structure and kinetic parameters than ends in elongation and shortening (Walker et al., 1989). As shown in Fig. 6, immediately after cutting, a severed end in the intermediate state has the lattice structure of the GDP-tubulin core of the microtubule, in contrast to the elongation state, where ends are capped with GTP-tubulin or GDP-P_i-tubulin (Caplow et al., 1989; Melki et al., 1990; Stewart et al., 1990; Voter et al., 1991; Walker et al., 1991; Hyman et al., 1992; Drechsel and Kirschner, 1994; Caplow and Shanks, 1996; Melki et al., 1996), and the shortening state, where ends are capped with inside-out peeling GDP-tubulin protofilaments (Erickson, 1974, 1975; Kirschner et al., 1974, 1975*a*,*b*; Simon and Salmon, 1990; Mandelkow et al., 1991; Chrétien et al., 1995; Erickson and Stoffler, 1996; Tran et al., 1997). This intermediate state makes both spontaneous catastrophe and rescue two-step processes in which the kinetic parameters can differ between the two ends.

In the three-state conformational cap model in Fig. 6, the first step of catastrophe for either end depends on the loss of a GTP cap. The elongation (E) state is stabilized by strong lateral interactions between the GTP-tubulin dimers, which are thought to have a "straight" conformation (Simon and Salmon, 1990; Mandelkow et al., 1991; Chrétien et al., 1995; Tran et al., 1997). The loss of the GTP cap either spontaneously (k_{EI}) or by cutting produces an intermediate state (I) with a GDP-tubulin end and the lattice structure of the core of the microtubule. The lateral interactions between these GDP-tubulins is thought to be weaker than those of GTP-tubulin because hydrolysis of the β tubulin GTP has induced conformational changes in β tubulin that strains

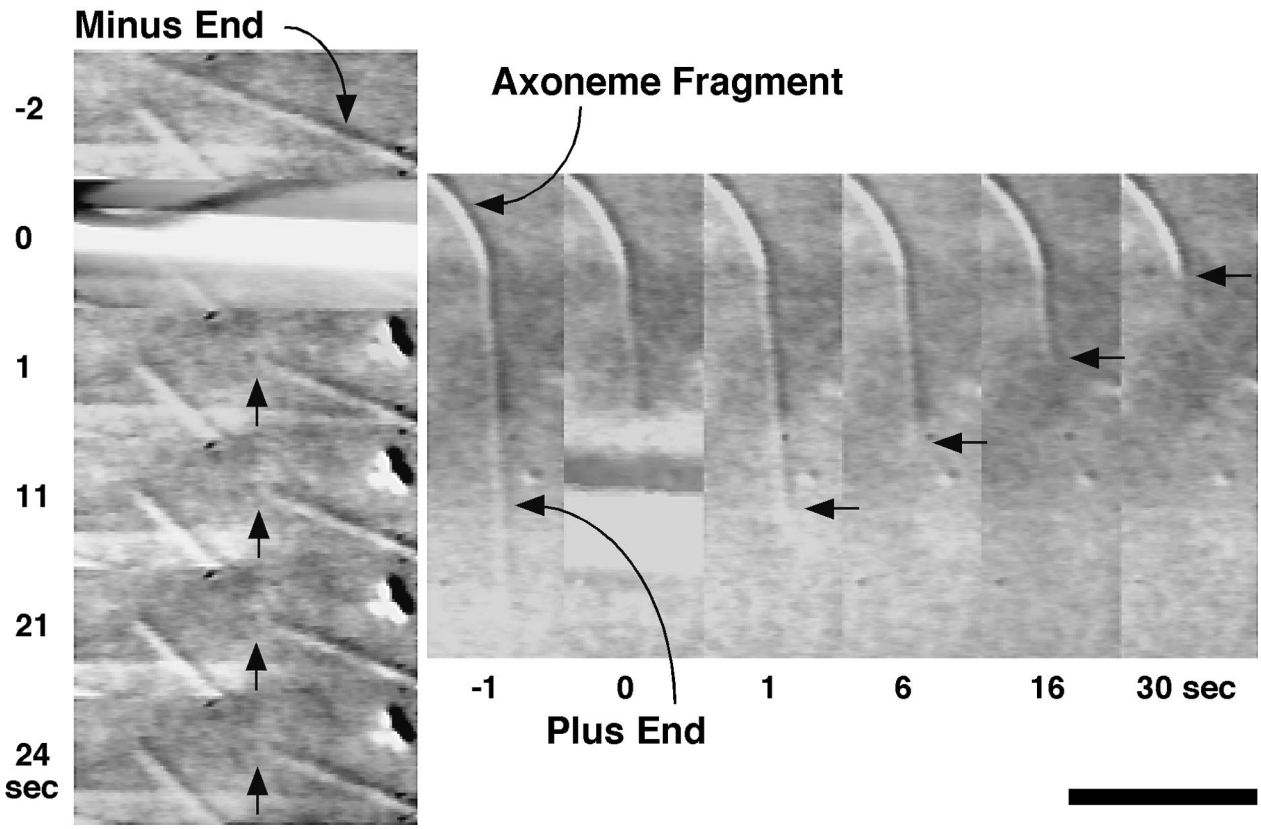

Figure 5. Glass microneedle severing of axoneme-nucleated microtubules. Sequence showing the behaviors typical of severed plus and minus ends. After severing, the plus end immediately and rapidly shortened back to the axoneme; the minus end continued growing without rapid shortening. Bar, 10 μm.

or kinks the dimer (Melki et al., 1989; Hyman et al., 1995). From this intermediate state, an end can revert back to the elongation state (k_{IE}) by reforming a GTP-tubulin cap either by addition of GTP-tubulin or by GTP exchange into GDP-dimers at the end (our results and Caplow and Shanks, 1996). For a catastrophe to occur, the end must switch (k_{IS}) to the shortening state (S), which most likely involves a structural transformation at the end of the polymer where the majority of terminal GDP-tubulin subunits curl inside-out, breaking their lateral bonds (Inoué and Salmon, 1995; Erickson and Stoffler, 1996; Tran et al., 1997). Once initiated, curling propagates rearward producing mi-

Table II. The Parameters of Pure Tubulin Microtubule Dynamic Instability at 16 μM GTP-tubulin, 1 mM Mg^{2+}-GTP, and 22°C, in vitro

	Plus ends (+)	Minus ends (−)
Elongation rate (μm/min)	1.37 ± 0.08 (n = 27)	0.41 ± 0.04 (n = 14)
Rapid shortening rate (μm/min)	22.16 ± 1.69 (n = 18)	28 ± 2.50 (n = 8)
Catastrophe frequency* (s^{-1})	0.0045	0.0011
Rescue frequency‡ (s^{-1})	0.002§	0.15

*Catastrophe frequency is calculated as number of transition events observed per total time spent in the growth phase. Total time observed was 4,494 s for the plus end and 7,453 s for the minus end (Walker et al., 1988).
‡Rescue frequency is calculated as number of transition events observed per total time spent in the shortening phase. Total time observed was 484 s for the plus end and 48 s for the minus end (Walker et al., 1988).
§Only one rescue was observed during 484 s of rapid shortening.
Note: Some of the above values were reported previously in Walker et al., 1989, but are included here for completeness.

Table III. Summary of the Mechanical Microneedle Severing of Axoneme-nucleated Microtubules

	Plus ends (+)	Minus ends (−)
16 μM GTP-tubulin, 1 mM Mg^{2+}-GTP		
n	140	132
Shortened	99.3%	22%
Stable	0.7%	78%
32 μM GTP-tubulin, 1 mM Mg^{2+}-GTP		
n	44	57
Shortened	91%	3.5%
Stable	9%	96.5%
2 μM GTP-tubulin, 1 mM Mg^{2+}-GTP		
n	79	49
Shortened	0	0
Stable	100%	100%
50 μM Sephadex-treated GTP-tubulin, no Mg^{2+}-GTP		
n	0*	106
Shortened	n.a.	72%
Stable	n.a.	28%

*No microtubules were able to polymerize at the plus ends of axonemes.

crotubule shortening through rapid dimer dissociation and breakage of the curved protofilaments. It is possible that cutting opens up the microtubule cylinder, creating plus and minus severed ends with sheets like those observed for rapidly growing ends where tubulin protofilament sheets have not yet folded up at the seam to form the cylindrical microtubule (Simon et al., 1991; Chrétien et al., 1995). But, the point of the intermediate state in Fig. 6 is that the ends are GDP-tubulin with lateral protofilament interactions similar to the microtubule core and would not contain the GTP-tubulin of growing ends nor the inside-out curled GDP-tubulin protofilaments at shortening ends (Fig. 6).

The transition rate constants, k_{EI} and k_{IE} (Fig. 6), are expected to depend on the concentrations of Mg^{2+}-GTP and GTP-tubulin, with higher concentrations reducing the value of k_{EI} and increasing the value of k_{IE}. This is because higher tubulin concentrations reduce spontaneous catastrophe frequency (Walker et al., 1988), while lower concentrations of Mg^{2+}-GTP induce catastrophe (our results and Caplow and Shanks, 1995). In addition, we found that the percentage of stable severed ends, and hence k_{IE}, increases with higher GTP-tubulin concentration. The transition rate constant k_{IS} reflects only the structural transformation between the intermediate and shortening states and is not expected to depend on either GTP-tubulin or Mg^{2+}-GTP concentrations.

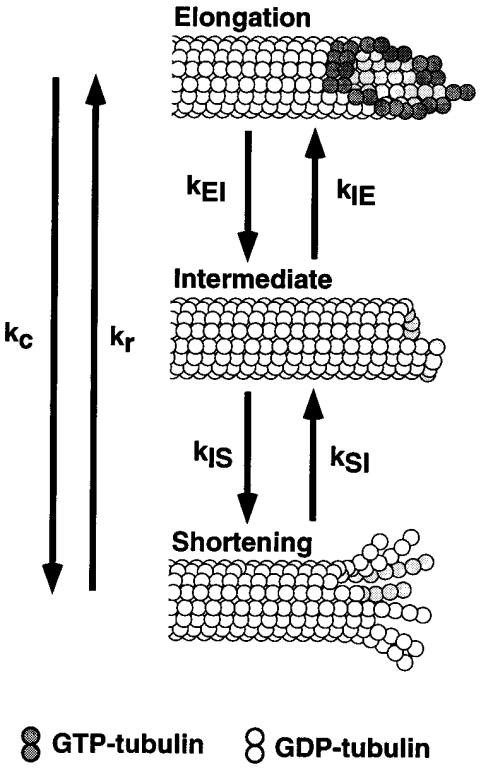

Figure 6. In the three-state model of dynamic instability, k_c is the frequency of spontaneous catastrophe, k_r is the frequency of spontaneous rescue, k_{EI} is the frequency of transition between elongation (E) and the intermediate state (I), k_{IE} is the frequency of transition from I to E, k_{IS} is the frequency of transition from I to S, and k_{SI} is the frequency of transition from S to I. Note that each of these transition rate constants corresponds to changes in the structure of the microtubule ends as described in the text.

Rescue is also a two-step process in this model (Fig. 6). First, the end must make a structural transformation (k_{SI}) from the shortening to the intermediate state. From this intermediate state, the end can either regain its GTP-tubulin cap (k_{IE}) and achieve rescue or switch back to shortening (k_{IS}), without rescue. The transition rate constant in this model is assumed to be independent of GTP-tubulin and Mg^{2+}-GTP concentrations since it only involves the structural transformation from the shortening to the intermediate state. This may be an over simplification since the addition of GTP-tubulin dimers to the ends of short curled protofilaments at shortening ends could promote lateral bond formation and the transformation either to an intermediate state end or a recapped growing end.

The Kinetic Behavior of the Intermediate State at Plus and Minus Ends Is Different

In the three-state conformational cap model (Fig. 6), the behavior of a severed end in the intermediate state will depend on the probabilities of conversion from the intermediate state to either the elongation or shortening states. The probability, P_{IS}, of a severed end converting to a shortening end rather than reverting back to a growing end is given by the percentage of severed ends that shortened at each end in our severing experiments (Table I) and depends on k_{IE} and k_{IS} by $P_{IS} = k_{IS}/(k_{IE} + k_{IS})$ (see Appendix). At 16 μM tubulin, $P_{IS} = 0.993$ for severed plus ends and $P_{IS} = 0.22$ for severed minus ends. At plus ends, the conversion from the intermediate state to shortening is highly favored ($k_{IE} \gg k_{IS}$) since the great majority of severed plus ends are not stable. In contrast, at minus ends, conversion from the intermediate state to elongation is favored ($k_{IE} > k_{IS}$) since the great majority of severed minus ends are stable. In fact, while in the intermediate state at 16 μM tubulin, plus ends are 141 times more likely to switch to the shortening state than to revert to elongation. But, for the minus ends in the intermediate state, they are 3.5 times more likely to revert to elongation rather than switch to the shortening state.

This analysis predicts that plus ends rarely lose their GTP-tubulin cap without converting to rapid shortening, but minus ends often lose and regain their GTP caps a number of times before a catastrophe finally occurs. Conversely, plus ends convert from the shortening to the intermediate state and back many times before a rescue occurs, while minus ends achieve rescue for almost every switch from shortening to the intermediate state. The frequent conversion to the intermediate state and back to the shortening state by plus ends would slow down the rate of shortening and help explain why the rate of shortening of plus ends is typically slower than for minus ends (Table II and Walker et al., 1988, 1989).

In the Appendix, we derive equations relating the frequencies of catastrophe and rescue to the four transition rate constants in the three-state model and use these equations to calculate approximate values for plus and minus ends from our measured values for catastrophe, rescue, and the fraction of stable severed ends (Fig. 7). A major point that can be seen by comparing the kinetic parame-

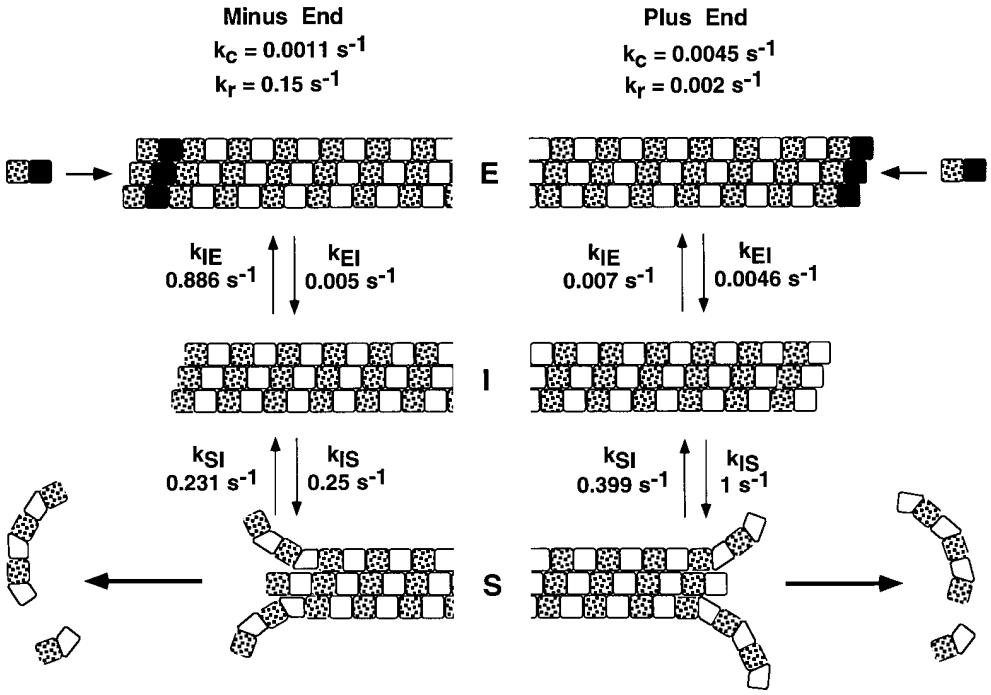

Figure 7. The opposite orientation of tubulin dimers at plus and minus ends is probably responsible for the differences in dynamic instability as described in the text. The values of the frequencies of catastrophe, k_c, and rescue, k_r, are taken from Table II for 16 μM tubulin. The values for the transition rate constants at each end were calculated as described in the Appendix.

ters in Fig. 7 is that the biggest difference between plus and minus ends is the value for the transition between the intermediate state and elongation, k_{IE}, which is 100-fold less for plus verses minus ends. Both ends lose their GTP caps (k_{EI}), switch from the intermediate state to shortening (k_{IS}), and switch from shortening back to the intermediate state (k_{IE}) at similar frequencies, indicating that the mechanisms involved with these transitions are similar for both ends. The big question, then, is what is different about the intermediate state at plus and minus ends that makes such an enormous difference in k_{IE}.

The Polarity of the Tubulin Dimer Is Likely Responsible for the Asymmetry in Plus and Minus End Dynamic Instability

The simplest explanation (Fig. 7) is that k_{IE} depends critically on the polarity of the αβ tubulin dimer in the microtubule lattice (Mandelkow and Mandelkow, 1990). Microtubules are polarized polymers of αβ tubulin dimers oriented head-to tail along each of the 13 protofilaments, which together compose the cylindrical wall of the microtubule. Each tubulin monomer is slightly staggered relative to its lateral neighbors in a 3-start left-handed helix. The protofilaments are held together in the cylindrical microtubule wall by lateral α–α and β–β bonds except at a "seam" between two protofilaments where α–β and β–α lateral bonds occur (for reviews see Erickson and Stoffler, 1996; Wade and Chrétien, 1993). The plus and minus ends of a microtubule are different because one end contains dimers oriented with α tubulin outwards, while the other end contains dimers with β tubulin oriented outwards. The orientation of the dimers at plus and minus ends has been controversial (Erickson and Stoffler, 1996), but recently Amos and co-workers have provided convincing structural evidence that the plus end contains a crown of β tubulin, while the minus end contains a crown of α tubulin (Fan et al., 1996).

This orientation of the tubulin dimer provides a structural explanation for the different behavior of severed plus and minus ends. Severed plus ends in the intermediate state contain crowns of β tubulin containing bound GDP (Caplow and Shanks, 1996). Since solution GDP-tubulin promotes catastrophe (Caplow and Shanks, 1995; Vandecandelaere et al., 1995), the conformational changes in β tubulin associated with GTP hydrolysis are likely to inhibit binding of the terminal β subunit to the α end of a GTP-tubulin dimer in solution in comparison to the rate of dimer association for growing ends containing GTP-tubulin (Fig. 7, *Plus End*). This would significantly reduce the probability of recapping. In contrast, severed minus ends in the intermediate state contain crowns of α tubulin with bound GTP, much like the terminal α tubulins at growing minus ends. The terminal orientation of α tubulin provides efficient association with the β tubulin end of a free GTP-tubulin dimer and quick recapping (Fig. 7; *Minus End*). In addition, the terminal β tubulins at severed plus ends are more likely to curl inside-out, switching the ends to the shortening state, since they have hydrolyzed their GTP. In comparison, the terminal α tubulins at severed minus ends always contain GTP and as a result achieve stronger lateral interaction, making the ends more stable and capable of binding GTP-tubulin.

The dimer polarity in the microtubule lattice also provides an explanation for why depletion of free GTP affects the stability of both ends, but to a greater extent at the plus end. Even at the 50 μM tubulin concentrations in our experiments, plus ends, but not minus ends, were unstable and quickly converted to shortening within several seconds when the free GTP was depleted. Thus, growing plus ends require free GTP to stabilize the GTP cap, presumably because the terminal β tubulins favor GTP exchange,

as shown by Mitchison (1993) based on the preferential binding of GTP bound beads to plus ends. In contrast, minus end stability was much less sensitive to depletion of free GTP in Caplow and Shank's (1995) and our experiments, and Mitchison (1993) found little binding of the GTP-bound beads to minus ends. A remarkable result in our experiments was the significant percentage of minus severed ends that remained stable in buffers with depleted Mg^{2+}-GTP. We attribute this stability to the crown of α tubulin at minus ends.

The 50 μM Sephadex–treated tubulin in our experiments contains GTP-tubulin in a 1:1 complex, without any added Mg^{2+}-GTP. The K_d of GTP-tubulin is 22 nM (Zeeberg and Caplow, 1979), leading to a 1 μM equilibrium concentration of free GTP and 1 μM tubulin without GTP bound at the exchangeable β subunit, or "apo-tubulin" (Caplow and Shanks, 1995). Thus, 2% of the 50 μM tubulin is apo-tubulin. It is possible that this apo-tubulin may contribute to the marked decrease in stability at the plus end before severing and the minus end after severing (see Caplow and Shanks, 1995). The observation that low or no free solution Mg^{2+}-GTP decreased the stability of severed minus ends implies that GTP exchange at the minus ends is occurring, but at a much slower rate than at the plus ends.

Other Potential Contributions of the Intermediate State

From careful analysis of the frequency of catastrophe as a function of the duration of microtubule elongation, Odde et al. (1995) have found that spontaneous catastrophe of pure tubulin microtubules in vitro is a multistep process, as predicted by our three-state model. In addition, growing and shortening ends in vitro have been observed to pause or hesitate briefly several times before either a catastrophe or rescue occurs (Horio and Hotani, 1986; Schulze and Kirschner, 1987; Walker et al., 1988; Shelden and Wadsworth, 1992). These pauses could represent periods when ends are in the intermediate state.

In living cells, severing microtubules with UV or laser microbeams or microneedle has been reported to produce labile plus ends that shorten to various extents and stable severed minus ends (Leslie and Pickett-Heaps, 1984; Nicklas et al., 1989; Tao et al., 1988; Wilson and Forer, 1988; Spurck et al., 1990; Izutsu and Suto, 1992). This behavior is predicted from the differential stability of plus and minus severed ends in our in vitro experiments and those of Walker et al. (1989). There also appear to be factors in the cytoplasm that selectively stabilize either plus or minus ends (Gard and Kirschner, 1987; Gliksman et al., 1992; Gundersen et al., 1994; Vasquez et al., 1994; Parsons and Salmon, 1997) and prevent their elongation or shortening. Since neither elongation nor shortening is reported to occur at these stable ends, they could be similar in structure to the intermediate state identified in our experiments, and the stabilizing factors could be specifically binding to these ends because they are in the intermediate state. The movements of kinetochores in vertebrate tissue cells is tightly coupled to changes in the assembly/disassembly of kinetochore microtubules at their plus end kinetochore attachment sites (for review see Inoué and Salmon, 1995). The intermediate state may play an important role in regulating force production and the direction of kinetochore movement (Skibbens et al., 1993; Rieder and Salmon, 1994; Inoué and Salmon, 1995; Khodjakov and Rieder, 1996).

At low concentrations, several microtubule assembly inhibitors, including vinblastine and nocodazole, greatly suppress the dynamic instability of microtubule plus ends for microtubules assembled with microtubule-associated proteins in vitro (Faruki et al., 1992; Wilson and Jordan, 1994; Parsons and Salmon, 1997) or for cytoplasmic microtubules in interphase tissue cells (Dhamodharan et al., 1995). It may be that the drug–tubulin complexes stabilize the intermediate state as well as prevent elongation. These drugs also produce a mitotic block, which is important in cancer cell treatment (Jordan et al., 1992), and this block could be a consequence of stabilization of plus ends in the intermediate state.

Appendix

Derivation of the Equations Relating Catastrophe and Rescue to the Four Transition Rate Constants for the Three-State Model

Consider the intermediate state I. I has two possible reaction pathways, that of transition to E or that of transition to S, as follows:

$$\mathrm{E} \underset{k_{IE}}{\longleftarrow} \mathrm{I} \underset{k_{IS}}{\longrightarrow} \mathrm{S},$$

where k_{IE} and k_{IS} are rates of transitions, or the number of events per unit time. The total number of events/s that I can have is $(k_{IE} + k_{IS})$, and the probability of switching from I to S is

$$P_{IS} = k_{IS}/(k_{IE} + k_{IS}), \tag{A1}$$

and the probability of switching from I to G is

$$P_{IE} = k_{IE}/(k_{IE} + k_{IS}). \tag{A2}$$

An elongating microtubule end initially makes a transition to the I state. Once in the I state, it can either convert to the S state or revert back to the E state without ever shortening:

$$\mathrm{E} \underset{k_{IE}}{\overset{k_{EI}}{\rightleftarrows}} \mathrm{I} \overset{k_{IS},\ k_c}{\longrightarrow} \mathrm{S}$$

The catastrophe frequency k_c is mathematically related to k_{EI}, k_{IE}, and k_{IS}. Think in terms of the mean times required for the transition between the E, I, and S states. The reciprocal of catastrophe is the mean elongation duration, t_{ES}, before conversion from E to the S state, or

$$t_{ES} = 1/k_c. \tag{A3}$$

When in the E state, the mean time, t_{EI}, for transition into the I state is given by the reciprocal of k_{EI}:

$$t_{EI} = 1/k_{EI}. \tag{A4}$$

Once in the I state, the mean duration, t_Δ, before either converting to S or back to E is given by,

$$t_\Delta = 1/(k_{IE} + k_{IS}). \quad \text{(A5)}$$

Now, the time spent in the E and I state before converting to S, t_{ES}, is the sum ($t_{EI} + t_\Delta$) multiplied by the number of switches to I before a switch to S occurs, $1/P_{IS}$, or

$$t_{ES} = (t_{EI} + t_\Delta)/P_{IS}. \quad \text{(A6)}$$

We can now solve for k_c in terms of k_{EI}, k_{IE}, and k_{IS} by substituting Eqs. A3, A4, and A5 into A6:

$$k_c = k_{EI}k_{IS}/(k_{EI} + k_{IE} + k_{IS}). \quad \text{(A7)}$$

The derivation of the equation that relates the rescue frequency, k_r, to the transition rate constants follows similar logic to that used above for catastrophe. The concept is that an S end makes a transition to an I state. Once in the I state, it either converts to the E state or reverts back to the S state without ever growing. Therefore, for rescue, three rate constants are involved:

$$\begin{array}{ccccc} & & \xrightarrow{\quad k_r \quad} & & \\ & k_{SI} \swarrow & & \searrow k_{IE} & \\ S & \longleftrightarrow & I & \longrightarrow & E \\ & k_{IS} \searrow & & & \end{array}$$

Following the same reasoning as used to derive Eq. A7, rescue is given by

$$k_r = k_{SI}k_{IE}/(k_{SI} + k_{IS} + k_{IE}). \quad \text{(A8)}$$

Calculation of Approximate Values for the Transition Rate Constants

We have measured values for catastrophe and rescue frequencies at 16 μM tubulin. Because only three equations (A1, A2, and A3) are available for the four unknown transition rate constants, we cannot explicitly solve for them. However, minimal values for k_{IS} can be obtained from the delay in rapid shortening that occurs when growing ends are rapidly diluted. They have been estimated to switch to shortening after a delay of ~1 s for plus and ~4 s for minus for dilution to zero GTP-tubulin concentration (Walker et al., 1991). From these dilution results, the minimal values for k_{IS} are $k_{IS} = 1\ s^{-1}$ for plus and $0.25\ s^{-1}$ for minus ends.

Substituting these k_{IS} values into Eqs. A1, A2, and A3 yields the four rate constants for 16 μM tubulin and 1 mM Mg^{2+}-GTP at 22°C given in Fig. 7. We found that increasing the values of k_{IS} 10-fold for either the plus or minus ends increases the values of k_{IE} in proportion (Eq. A1), but has relatively little effect on the calculated values of k_{EI} and k_{SI}. Thus, the values in Fig. 7 provide a good first approximation to the values of k_{EI} and k_{SI} and a framework for discussion of the kinetic differences between plus and minus ends.

We gratefully acknowledge Drs. R.B. Nicklas and D.H. Zhang for their expert advice on pulling needles, Dr. M. Caplow and J. Shanks for their generous gift of GMPCPP and assistance with handling [^{32}P]GTP, and V.P. Skeen for her assistance in phosphocellulose-tubulin purification.

This work was supported by National Institutes of Health grant GM 24364 to E.D. Salmon.

Received for publication 13 January 1997 and in revised form 29 April 1997.

References

Begg, D.A., and G.W. Ellis. 1979. Micromanipulation studies of chromosome movement. I. Chromosome-spindle attachment and the mechanical properties of chromosomal spindle fibers. *J. Cell Biol.* 82:528–541.

Bell, C.W., C. Fraser, W.S. Sale, W.-J.Y. Tang, and I.R. Gibbons. 1982. Preparation and purification of dynein. *Methods Cell Biol.* 24:373–397.

Billger, M.A., G. Bhatacharjee, and R.C. Williams, Jr. 1996. Dynamic instability of microtubules assembled from microtubule-associated-protein-free tubulin: neither variability of growth and shortening rates nor "rescue" requires microtubule-associated proteins. *Biochemistry.* 35:13656–13663.

Caplow, M. 1992. Microtubule dynamics. *Curr. Opin. Cell Biol.* 4:58–65.

Caplow, M., and J. Shanks. 1995. Induction of microtubule catastrophe by formation of tubulin-GDP and apotubulin subunits at microtubule ends. *Biochemistry.* 34:15732–15741.

Caplow, M., and J. Shanks. 1996. Evidence that a single monolayer tubulin-GTP cap is both necessary and sufficient to stabilize microtubules. *Mol. Biol. Cell.* 7:633–675.

Caplow, M., R. Ruhlen, J. Shanks, R.A. Walker, and E.D. Salmon. 1989. Stabilization of microtubules by tubulin-GDP-Pi subunits. *Biochemistry.* 28:8136–8141.

Caplow, M., R.L. Ruhlen, and J. Shanks. 1994. The free energy for hydrolysis of a microtubule-bound nucleotide triphosphate is near zero: all of the free energy for hydrolysis is stored in the microtubule lattice [erratum published 1995, 129:549]. *J. Cell Biol.* 127:779–788.

Carlier, M.F., and D. Pantaloni. 1978. Kinetic analysis of cooperativity in tubulin polymerization in the presence of guanosine di- or triphosphate nucleotides. *Biochemistry.* 17:1908–1915.

Carlier, M.-F., and D. Pantaloni. 1981. Kinetic analysis of guanosine 5′-triphosphate hydrolysis associated with tubulin polymerization. *Biochemistry.* 20: 1918–1924.

Carlier, M.F., R. Melki, D. Pantaloni, T.L. Hill, and Y. Chen. 1987. Synchronous oscillations in microtubule polymerization. *Proc. Natl. Acad. Sci. USA.* 84:5257–5261.

Chrétien, D., S.D. Fuller, and E. Karsenti. (1995). Structure of growing microtubule ends: two-dimensional sheets close into tubes at variable rates. *J. Cell Biol.* 129:1311–1328.

David-Pfeuty, T., H.P. Erickson, and D. Pantaloni. 1977. Guanosinetriphosphatase activity of tubulin associated with microtubule assembly. *Proc. Nat. Acad. Sci. USA.* 74:5372–5376.

Dhamodharan, R., M.A. Jordon, D. Thrower, L. Wilson, and P. Wadsworth. 1995. Vinblastine suppresses dynamics of individual microtubules in living interphase cells. *Mol. Biol. Cell.* 6:1215–1229.

Drechsel, D.N., and M.W. Kirschner. 1994. The minimum GTP cap required to stabilize microtubules [erratum published 1995, 5:215]. *Curr. Biol.* 4:1053–1061.

Erickson, H.P. 1974. Assembly of microtubules from preformed, ring-shaped protofilaments and 6-S tubulin. *J. Supramol. Struct.* 2:393–411.

Erickson, H.P. 1975. The structure and assembly of microtubules. *Ann. New York Acad. Sci.* 253:60–77.

Erickson, H.P., and E.T. O'Brien. 1992. Microtubule dynamic instability and GTP hydrolysis. *Ann. Rev. Biophys. Biomol. Struct.* 21:145–66.

Erickson, H.P., and D. Stoffler. 1996. Protofilaments and rings, two conformations of the tubulin family conserved from bacterial FtsZ to α/β and γ tubulin. *J. Cell Biol.* 135:5–8.

Fan, J., A.D. Lockhart, R.A. Cross, and L.A. Amos. 1996. Labelling of microtubule minus ends with a phage display antibody to an N-terminal epitope of alpha tubulin. *J. Mol. Biol.* 259:325–330.

Faruki, S., M. Doree, and E. Karsenti. 1992. cdc2 kinase-induced destabilization of MAP2-coated microtubules in *Xenopus* egg extracts. *J. Cell Sci.* 101:69–78.

Fygenson, D.K., E. Braun, and A. Lichaber. 1994. Phase diagrams of microtubules. *Phys. Rev. E.* 50:1579–1588.

Gard, D.L., and M.W. Kirschner. 1987. A microtubule-associated protein from *Xenopus* eggs that specifically promotes assembly at the plus-end. *J. Cell Biol.* 105:2203–2215.

Gliksman, N.R., S.F. Parsons, and E.D. Salmon. 1992. Okadaic acid induces interphase to mitotic-like microtubule dynamic instability by inactivating rescue. *J. Cell Biol.* 119:1271–1276.

Gundersen, G.G., I. Kim, and C.J. Chapin. 1994. Induction of stable microtubules in 3T3 fibroblasts by TGF-β and serum. *J. Cell Sci.* 107:645–659.

Horio, T., and H. Hotani. 1986. Visualization of the dynamic instability of individual microtubules by dark-field microscopy. *Nature (Lond.).* 321:605–607.

Hyman, A.A., and E. Karsenti. 1996. Morphogenetic properties of microtubules and mitotic spindle assembly. *Cell.* 84:401–410.

Hyman, A.A., S. Salser, D.N. Drechsel, N. Unwin, and T.J. Mitchison. 1992. Role of GTP hydrolysis in microtubule dynamics: information from a slowly

hydrolyzable analogue, GMPCPP. *Mol. Biol. Cell.* 3:1155–1167.
Hyman, A.A., D. Chretien, I. Arnal, and R.H. Wade. 1995. Structural changes accompanying GTP hydrolysis in microtubules: information from a slowly hydrolyzable analogue guanylyl-(α,β)-methylene-diphosphonate. *J. Cell Biol.* 128:117–125.
Inoué, S., and E.D. Salmon. 1995. Force generation by microtubule assembly/disassembly in mitosis and related movements. *Mol. Biol. Cell.* 6:1619–1640.
Izutsu, K., and H. Sato. 1992. Rapid backward movement of anaphase chromosomes whose kinetochore fibers were cut by ultraviolet microbeam irradiation. *Biol. Cell.* 76:339–350.
Jameson, L., and M. Caplow. 1980. Effect of guanosine diphosphate on microtubule assembly and stability. *J. Biol. Chem.* 255:2284–2292.
Jordan, M.A., D. Thrower, and L. Wilson. 1992. Effects of vinblastine, podophyllotoxin and nocodazole on mitotic spindles. Implications for the role of microtubule dynamics in mitosis. *J. Cell Sci.* 102:401–416.
Kiehart, D.P. 1981. Studies on the in vivo sensitivity of spindle microtubules to calcium ions and evidence for a vesicular calcium-sequestering system. *J. Cell Biol.* 88:604–617.
Kirschner, M., and E. Schulze. 1986. Morphogenesis and the control of microtubule dynamics in cells. *J. Cell Sci.* 5(Suppl.):293–310.
Kirschner, M., R. Williams, M. Weingarten, and J. Gerhart. 1974. Microtubules from mammalian brain: some properties of their depolymerization products and a proposed mechanism of assembly and disassembly. *Proc. Nat. Acad. Sci. USA.* 71:1159–1163.
Kirschner, M.W., L.S. Honig, and R.C. Williams. 1975*a.* Quantitative electron microscopy of microtubule assembly in vitro. *J. Mol. Biol.* 99:263–276.
Kirschner, M.W., M. Suter, M. Weingarten, and D. Littman. 1975*b.* The role of rings in the assembly of microtubules in vitro. *Ann. New York Acad. Sci.* 253: 90–106.
Khodjakov, A., and C.L. Rieder. 1996. kinetochores moving away from their associated poles do not exert a significant pushing force on the chromosomes. *J. Cell Biol.* 135:315–327.
Leslie, R.J., and J.D. Pickett-Heaps. 1984. Spindle microtubule dynamics following ultraviolet-microbeam irradiations of mitotic diatoms. *Cell.* 36:717–727.
Mandelkow, E., and E.M. Mandelkow. 1990. Microtubular structure and tubulin polymerization. [Review]. *Curr. Opin. Cell Biol.* 2:3–9.
Mandelkow, E.M., E. Mandelkow, and R.A. Milligan. 1991. Microtubule dynamics and microtubule caps: a time-resolved cryo-electron microscopy study. *J. Cell Biol.* 114:977–991.
Melki, R., M.F. Carlier, D. Pantaloni, and S.N. Timasheff. 1989. Cold depolymerization of microtubules to double rings: geometric stabilization of assemblies. *Biochemistry.* 28:9143–9152.
Melki, R., M.F. Carlier, and D. Pantaloni. 1990. Direct evidence for GTP and GDP-Pi intermediates in microtubule assembly. *Biochemistry.* 29:8921–8932.
Melki, R., S. Fievez, and M.-F. Carlier. 1996. Continuous monitoring of Pi release following nucleotide hydrolysis in actin or tubulin assembly using 2-amino-6-mercapto-7-methylpurine ribonucleoside and purine-nucleoside phosphorylase as an enzyme-linked assay. *Biochemistry.* 35:12038–12045.
Mickey, B., and J. Howard. 1995. Rigidity of microtubules is increased by stabilizing agents. *J. Cell Biol.* 130:909–917.
Mitchison, T., and M. Kirschner. 1984. Dynamic instability of microtubule growth. *Nature (Lond.).* 312:237–242.
Mitchison, T.J. 1993. Localization of an exchangeable GTP binding site at the plus end of microtubules. *Science (Wash. DC).* 261:1044–1047.
Nicklas, R.B., G.M. Lee, C.L. Rieder, and G. Rupp. 1989. Mechanically cut mitotic spindles: clean cuts and stable microtubules. *J. Cell Sci.* 94:415–423.
O'Brien, E.T., and H.P. Erickson. 1989. Assembly of pure tubulin in the absence of free GTP: effect of magnesium, glycerol, ATP, and the nonhydrolyzable GTP analogues. *Biochemistry.* 28:1413–1422.
Odde, D.J., L. Cassimeris, and H.M. Buettner. 1995. Kinetics of microtubule catastrophe assessed by probabilistic analysis. *Biophys. J.* 69:796–802.
Parsons, S.F., and E.D. Salmon. 1997. Microtubule assembly in clarified *Xenopus* egg extracts. *Cell Motil. Cytoskel.* 36:1–11.
Rieder, C.L., and E.D. Salmon. 1994. Motile kinetochores and polar ejection forces dictate chromosome position on the vertebrate mitotic spindle. *J. Cell Biol.* 124:223–233.
Salmon, E.D., R.A. Walker, and N.K. Pryer. 1989. Video-enhanced differential interference contrast light microscopy. *Biotechniques.* 7:624–633.
Schulze, E., and M. Kirschner. 1987. Dynamic and stable populations of microtubules in cells. *J. Cell Biol.* 104:277–288.
Shelden, E., and P. Wadsworth. 1992. Microinjection of biotin-tubulin into anaphase cells induces transient elongation of kinetochore microtubules and reversal of chromosome-to-pole motion. *J. Cell Biol.* 116:1409–1420.
Simon, J.R., and E.D. Salmon. 1990. The structure of microtubule ends during the elongation and shortening phases of dynamic instability examined by negative-stain electron microscopy. *J. Cell Sci.* 96:571–582.
Simon, J.R., N.A. Adam, and E.D. Salmon 1991. Microtubule and tubulin sheet polymers elongate from isolated axonemes in vitro as observed by negative-stain electron microscopy. *Micron Microsc. Acta.* 22:405–412.
Skibbens, R.V., V.P. Skeen, and E.D. Salmon. 1993. Directional instability of kinetochore motility during chromosome congression and segregation in mitotic newt lung cells: a push-pull mechanism. *J. Cell Biol.* 122:859–875.
Spurck, T.P., O.G. Stonington, J.A. Snyder, H.J. Pickett, A. Bajer, and B.J. Mole. 1990. UV microbeam irradiations of the mitotic spindle. II. Spindle fiber dynamics and force production. *J. Cell Biol.* 111:1505–1518.
Stewart, R.J., K.W. Farrell, and L. Wilson. 1990. Role of GTP hydrolysis in microtubule polymerization: evidence for a coupled hydrolysis mechanism. *Biochemistry.* 29:6489–6498.
Tao, W., R.J. Walter, and M.W. Berns. 1988. Laser-transected microtubules exhibit individuality of regrowth, however most free new ends of the microtubules are stable. *J. Cell Biol.* 107:1025–1035.
Tran, P.T., P. Joshi, and E.D. Salmon. 1997. Structural dynamics of curved GDP-tubulin protofilaments at microtubule ends in the shortening state of dynamic instability. *J. Struct. Biol.* 118:107–118.
Vandecandelaere, A., S.R. Martin, and P.M. Bayley. 1995. Regulation of microtubule dynamic instability by tubulin-GDP. *Biochemistry.* 34:1332–1343.
Venier, P., A.C. Maggs, M.-F. Carlier, and D. Pantaloni. 1994. Analysis of microtubule rigidity using hydrodynamic flow and thermal fluctuations. *J. Biol. Chem.* 269:13353–13360.
Voter, W.A., and H.P. Erickson. 1984. The kinetics of microtubule assembly. Evidence for a two-stage nucleation mechanism. *J. Biol. Chem.* 259:10430–10438.
Voter, W.A., E.T. O'Brien, and H.P. Erickson. 1991. Dilution-induced disassembly of microtubules: relation to dynamic instability and the GTP cap. *Cell Motil. Cytoskel.* 18:55–62.
Wade, R.H., and D. Chrétien. 1993. Cryoelectron microscopy of microtubules. *J. Struct. Biol.* 110:1–27.
Walker, R.A., E.T. O'Brien, N.K. Pryer, M.F. Soboeiro, W.A. Voter, H.P. Erickson, and E.D. Salmon. 1988. Dynamic instability of individual microtubules analyzed by video light microscopy: rate constants and transition frequencies. *J. Cell Biol.* 107:1437–1448.
Walker, R.A., S. Inoué, and E.D. Salmon. 1989. Asymmetric behavior of severed microtubule ends after ultraviolet-microbeam irradiation of individual microtubules in vitro. *J. Cell Biol.* 108:931–937.
Walker, R.A., N.R. Gliksman, and E.D. Salmon. 1990. Using video-enhanced differential interference contrast microscopy to analyze the assembly dynamics of individual microtubules in real time. *In* Optical Microscopy for Biology. B. Herman and K. Jacobson, editors. Wiley-Liss, New York. 395–407.
Walker, R.A., N.K. Pryer, and E.D. Salmon. 1991. Dilution of individual microtubules observed in real time in vitro: evidence that cap size is small and independent of elongation rate. *J. Cell Biol.* 114:73–81.
Wilson, P.J., and A. Forer. 1988. Ultraviolet microbeam irradiation of chromosomal spindle fibres shears microtubules and permits study of the new free ends in vivo. *J. Cell Sci.* 91:455–468.
Wilson, L., and M.A. Jordan. 1994. Pharmacological probes of microtubule function. *In* Microtubules, J.S. Hyams and C.W. Lloyde, editors. Wiley-Liss, New York. 59–84.
Zeeberg, B., and M. Caplow. 1979. Determination of free and bound microtubular protein and guanine nucleotide under equilibrium conditions. *Biochemistry.* 18:3880–3886.